Desalination and Water Treatment
www.deswater.com
12 (2009) 3–15
1944-3994 / 1944-3986 © 2009 Desalination Publications. All rights reserved.
doi: 10.5004/dwt.2009.997

Iron(III) complex of an amino-functionalized poly(acrylamide)-grafted lignocellulosic residue as a potential adsorbent for the removal of chromium(VI) from water and industry effluents

Thayyath Sreenivasan Anirudhan*, Sreenivasan Rijith, Christu Das Bringle

Department of Chemistry, University of Kerala, Kariavattom, Trivandrum 695 581, India
Tel. +91 (471) 2418782; Fax +91 (471) 2307158; email: tsani@rediffmail.com

Received 19 July 2008; Accepted in revised form 10 November 2009

ABSTRACT

This study evaluated the effectiveness of a new adsorbent system (AM-Fe-PGCP), iron(III) complex of an amino-functionalized poly(acrylamide)-grafted coconut coir pith (CP) for the removal of chromium(VI) from aqueous solutions. The adsorbent was prepared through graft copolymerization of acrylamide onto CP in the presence of N,N′-methylenebisacrylamide using potassium peroxidisulphate initiator, followed by treatment with ethylenediamine and ferric chloride in acid (HCl) medium. The adsorbent was well characterized using FTIR, SEM, XRD, TG/DTG, surface area analyzer and potentiometric titrations. The ability of AM-Fe-PGCP to remove Cr(VI) from water and industrial effluent was tested using batch adsorption experiments. The effects of contact time, initial sorbate concentration, pH, dose of adsorbent and temperature were studied to optimize the conditions for maximum adsorption. The adsorption kinetics data were best described by the pseudo-second-order rate equation. The mechanism of sorption was found to be film diffusion controlled. Equilibrium isotherm data were analysed by the Langmuir and Freundlich equations. The best interpretation for the equilibrium data was given by the Langmuir isotherm and the maximum adsorption capacity was estimated to be 135.5 mg g^{-1} at 30°C. NaOH solution (0.1 M) was found to be capable of regenerating the spent adsorbent. Simulated industry wastewater sample was also treated by the AM-Fe-PGCP to demonstrate its efficiency in removing Cr(VI) from wastewater.

Keywords: Graft copolymers; Lignocellulosics; Adsorption; Chromium(VI); Thermodynamics; Desorption

1. Introduction

Chromium enters into the water bodies through activities associated with steel industry, electroplating, leather tanning, metal finishing, nuclear power plant, pigment and textile industries [1]. It occurs in Cr(III) and Cr(VI) forms. Cr(III) is an essential nutrient that potentiates insulin action and thus influences carbohydrate, lipid and protein metabolism. On the other hand, Cr(VI) is highly toxic to human beings and is classified as a human carcinogen. The maximum permissible levels of Cr(VI) in drinking and industrial wastewater were set by the EPA to be 0.05 and 0.20 mg/L, respectively [2]. Various methods have been developed for the removal of Cr(VI) from aqueous solutions such as ion exchange, reverse osmosis, adsorption, complexation and precipitation [3]. Compared with the other methods, adsorption is the most effective and widely used method. The potential of

* Corresponding author.

Presented at the Symposium on Emerging Trends in Separation Science and Technology (SESTEC-2008) March 12–14, 2008, University of Delhi, Delhi, India

using chemically modified lignocellulosics as adsorbents for water purification has been explored [4,5]. Lignocellulosics contain pectin and lignin which enhance the sorption potential due to the presence of surface hydroxyl and polyol groups. The application of lignocellulosics as such will cause certain problems such as lower durability, leaching of soluble organics and lower adsorption capacity. Earlier results demonstrated that chemical modifications such as esterification, quarternization, cross linking and grafting on biopolymers have improved their adsorption capacity and prevent the leaching of organics into solution. A number of ion exchange resins with different functionalities have been developed from certain lignocellulosic materials (e.g. orange residue saw dust, bagasse pith, banana stalk and banana stem) for the removal of heavy metals from aqueous solutions [6–10]. The suitability of lignocellulosic materials as precursors for graft polymerization is determined by their local and bulk availability. The coir process industry generates coir pith (CP) a lignocellulosic solid waste that presents a significant disposal problem. India, the third largest producer of coconut in the world, produces 7.5 million tons CP [11] as a waste generated in the process of separation of fiber from coconut husk. The results of the earlier studies showed that the product obtained from modified CP exhibits outstanding adsorption capacity for arsenic(V) from aqueous media [12,13]. In this work, we have prepared a novel adsorbent iron(III) complex of an amine-modified polyacrylamide grafted CP (AM-PGCP) by means of simple graft copolymerization reaction followed by loading with Fe(III) in the presence of HCl to utilize it for the effective removal of Cr(VI) from various aqueous media.

2. Experimental procedure

2.1. Preparation of adsorbent

The CP used for the preparation of adsorbent was procured from a local coir industry, and it was washed several times with distilled water to remove surface adhered particles and soluble materials. The oven dried CP was ground and sieved using standard test sieves to obtain the particle diameter of 0.096 mm. The composition of CP was determined using standard method described by Ott [14]. The amounts of α-cellulose, hemicellulose and lignin were found to be 46.1, 18.7 and 27.3%, respectively. Amine modified polyacrylamide grafted CP (AM-PGCP) was prepared according to our previous work [15]. Fig.1 represents the general procedure adopted for the preparation of adsorbent. 20 g of CP was immersed in 200 mL distilled water in 1 L reaction flask. About 5.0 g N,N′-methylenebisacrylamide, (MBA) as a cross linking agent and 1.0 g of potassium peroxydisulphate ($K_2S_2O_8$) as initiator were added to the above suspension and stirred well for 5 min at 250 rpm. Purified N_2 was passed through the vessel for 10 min. The polymerization was started by adding 25 g of acrylamide (AAM) monomer. The mixture was stirred at 250 rpm and 70°C in a water bath until a solid mass was obtained. The water soluble homopolymer was removed and the polyacrylamide

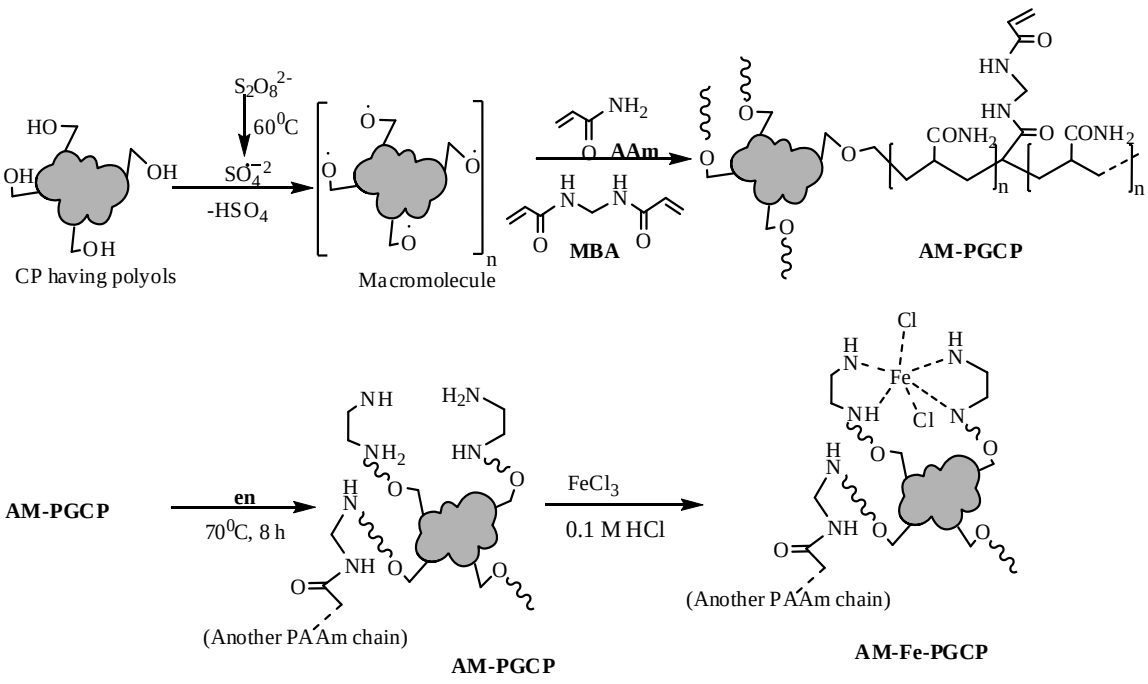

Fig. 1. Proposed mechanistic pathway for synthesis of AM-Fe-PGCP.

grafted CP (PGCP) obtained was collected. Grafting yield was determined as follows:

$$\text{Graft yield (\%)} = \frac{(w_1 - w_2) \times 100}{w_1} \quad (1)$$

where w_1 is the initial weight of the sample and w_2 is the grafted weight of the extracted sample. The grafting yield was found to be 78.8%. The dried mass was refluxed with 10 mL ethylenediamine (en) continuously for 8 h. The product, AM-PGCP was separated and washed with toluene and dried.

Design a batch operational condition at pH 3.0 to recognize maximum loading of iron(III) onto AM-PGCP based on the adsorption isotherm. The adsorption isotherm of iron(III) by AM-PGCP was determined by stirring 0.1 g of AM-PGCP at 250 rpm with 50 cm^3 iron(III) solution of concentration varying between 10 and 300 mg dm^{-3} at 30°C and pH 3.0. Sorption capacity (q_e) was calculated by the mass balance equation, $q = (C_0 - C_e)\, V/w$, where V, w, C_0, and C_e are the volume of solution (mL), the sorbent mass (g), and the initial and equilibrium concentrations (mg/L), respectively. The product, Fe(III)-loaded AM-PGCP (AM-Fe-PGCP) was filtered, washed with water and dried at 60°C for 24 h. The adsorbent thus obtained was ground using a mortar and pestle, and then sieved into particle sizes with an average diameter of 0.096 mm, represented as 80–230 mesh, using standard sieves. Several studies of adsorption onto various adsorbents have used a wide range of particle sizes (0.08–0.30 mm). Adsorbents with a small particle diameter have been reported for the high potentials of adsorption, principally due to large external surface areas and greater accessibility of the adsorption sites. In the present work, the adsorbent with an average particle size of 0.096 mm was used for adsorption experiments.

2.2. Equipment and method of characterization

The IR spectra of the CP and AM-Fe-PGCP were recorded on a Schimadzu FTIR spectrophotometer model 1801 using pressed disk technique. A potentiometric titration method [16] was used to determine the pH of point of zero charge (pH_{pzc}). Residual chromium(VI) concentrations after adsorption were analyzed spectrophotometrically [17] by monitoring the absorbance using UV-Visible spectrophotometer (Jasco model V 530). The XRD patterns of the adsorbent samples were obtained with a Siemens D 5005 X-ray unit using Ni-filtered Cu K_α radiation. Thermal stability of the absorbents was studied with a Mettler Toledo Stare thermo gravimetric analyzer. A scanning electron microscope (Polaron SC 7620) operated at 12 kV was used to study the surface morphology. The apparent density of the adsorbents was determined using a pycnometric method. The pH of the suspension was checked by using a Systronic (India) microprocessor pH meter (model μ362). A Labline (India) temperature controlled water bath shaker with a temperature tolerance of ±1.0°C was used in the equilibrium studies. The concentration of iron(III) in the solution was determined using a GBC Avanta-A5450 atomic absorption spectrophotometer (AAS). The following titrimetric procedure was employed to estimate the amine content of the AM-PGCP. About 0.1 g AM-PGCP was equilibrated with 25 mL 0.1 M HCl. After 24 h shaking, the adsorbent was collected by filtration, washed with distilled water to remove unreacted HCl. Filtrate was titrated against standard 0.1 M NaOH using phenolphthalein as indicator.

2.3. Adsorption experiments

A stock solution of 1000 mg L^{-1} was prepared by dissolving an appropriate amount of $K_2Cr_2O_7$. The solution was further diluted to the required concentrations before use. Batch adsorption experiments were conducted by shaking the flasks (100 mL capacity) for a period of time using a water bath shaker. AM-Fe-PGCP (0.1 g) was added to 50 mL Cr(VI) solution containing various concentrations and the contents were shaken at 30°C and 200 rpm. The initial pH of the solutions was adjusted by using 0.1 M HCl or 0.1 M NaOH. When the adsorption equilibrium was reached (2 h) the solid phase was separated by centrifugation at 1000 rpm for 10 min. The concentration of the Cr(VI) remaining in the supernatant was determined spectrophotometrically using 1,2-diphenyl carbazide as a chromogenic reagent. The amount adsorbed was measured from the difference between the Cr(VI) concentration in the initial and equilibrium states. The investigation for the effect of solution pH values on chromium adsorption was conducted at an initial chromium concentration of 50 and 100 mg/L, but the pH value ranged from 2.0 to 10.0. The adsorption kinetics was determined at pH 4.0 using different initial concentrations ranging from 100 to 250 mg L^{-1}. Samples were taken at different time intervals and the amount adsorbed was determined. Adsorption isotherms affected by temperatures were carried out at a pH of 4.0 by adding 2.0 g L^{-1} of AM-Fe-PGCP into 50 mL Cr(VI) solution with initial concentrations varying from 100 to 600 mg L^{-1}. The temperature was controlled in water bath shaker at the temperature ranged from 30 to 60 °C. After equilibrium the concentration of residual Cr(VI) ions in solution was analysed.

Cr(VI) reacts with 1,2-diphenylcarbazide in acid medium to form a red-violet coloured complex which is measured at 540 nm against a reagent blank carried through the same procedure. The minimum detectable concentration corresponding to 0.01 absorbance or 98% transmittance is 5 mg Cr(VI) when a 1.0 cm cell is used. The molar absorptivity is about 38462 L g^{-1} cm^{-1} at 540 nm with a sensitivity of 20 μg L^{-1}.

2.4. Desorption and regeneration studies

Desorption studies were conducted by batch experi-

ments. After performing adsorption experiments with 100 mg L^{-1} of Cr(VI) solution; the Cr(VI) loaded adsorbent was separated. The spent adsorbent was gently washed with distilled water to remove unadsorbed Cr(VI) ions. The exhausted adsorbent was added to desorption medium (0.1 M NaOH) and shaken for 3 h. After equilibrium, the suspension was centrifuged and the concentration of Cr(VI) in supernatant was analysed. Determine the amount of desorbed Cr(VI) ions onto solution. The adsorbent was subjected to the subsequent Cr(VI) loading cycle. Adsorption–desorption cycles up to four times were repeated to check the long term adsorption performance of AM-Fe-PGCP. All experiments and measurements were carried out in duplicate. The difference in results for the duplicates was typically less than 4.5 %.

3. Results and discussion

3.1. Adsorbent characterization

The FTIR spectra of pure CP, AM-PGCP, AM-Fe-PGCP and Cr(VI)- adsorbed AM-Fe-PGCP are shown in Fig. 2. From the spectrum of CP it shows a strong absorption band at 3280 cm^{-1} due to the hydrogen bonded stretching vibration from cellulose structure of the original CP. The pronounced peaks appeared at 1782 and 538 cm^{-1} are attributed to C=O stretching of hemicellulose and β-glycosidic linkages in CP. In addition, absorption bands at 2922 and 1028 cm^{-1} are assigned to the stretching and bending modes of methylene C–H groups present in CP. Involvement of hydroxyl groups for acrylamide grafting was confirmed by the observed shifting of stretching frequency corresponds to 3280 cm^{-1} in CP to 3740 cm^{-1} in AM-PGCP. The absorption bands arise at 3315 and 1665 cm^{-1} are characteristic to those N–H (stretching) and –C=O vibrations, respectively, from the amide group. Other peaks at 1620 and 1060 cm^{-1} correspond to N–H bending and C–N stretching vibrations from ethylenediamine bonded to the PGCP resulting through transamidation reaction. These results clearly indicate the presence of amine functionality in the AM-PGCP and provide evidence for grafting of AAM onto CP. The frequency shifts from 1620 to 1598 cm^{-1} and from 3315 to 3291 cm^{-1} confirm the involvement of amine groups for Fe(III) coordination. The band at 448 cm^{-1} is due to Fe–N stretching vibrations. Upon coordination the peak found at 1551 cm^{-1} shifted to 1536 cm^{-1} indicates the weakening of N–H bond in ethylenediamine moiety. These results clearly indicate the involvement of amine groups for Fe(III) binding. In the spectrum of the Cr(VI)-adsorbed AM-Fe-PGCP, peaks at 783 and 906 cm^{-1} are attributed to the Cr–O and Cr=O bonds from the chromate species, which suggests that Cr(VI) is adsorbed on the surface and the nitrogen atoms on the AM–Fe–PGCP is not involved in the adsorption. On comparing the spectrum of AM-Fe-PGCP with that of Cr(VI)-adsorbed AM-Fe-PGCP, it can be concluded that no chemical bond formation between the Cr(VI) species and the nitrogen atoms on the frame work, because it remained the same and was not shifted after adsorption process.

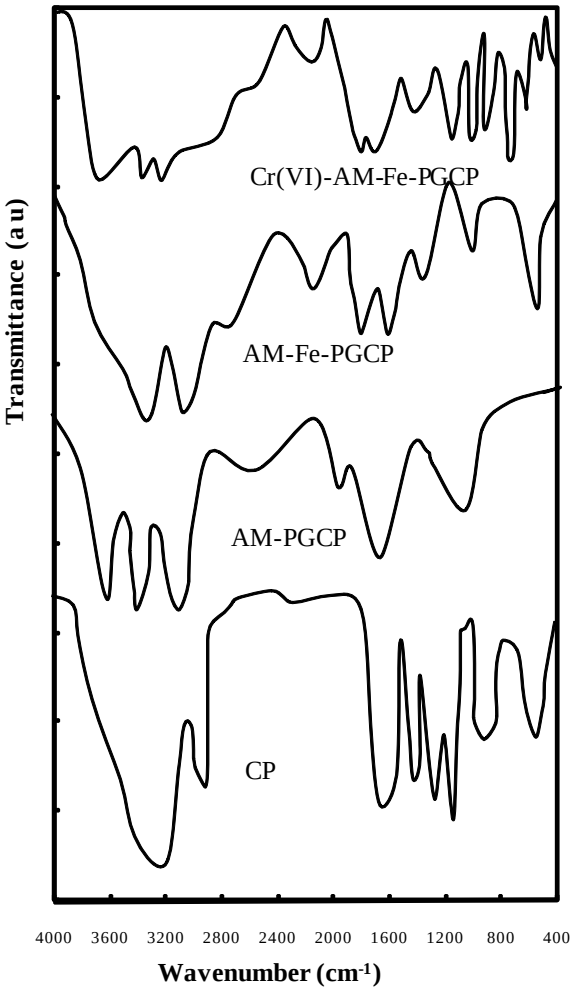

Fig. 2. FTIR spectra of CP, AM-PGCP, AM-Fe-PGCP and Cr(VI)-AM-Fe-PGCP.

The surface morphologies of the CP, AM-PGCP and AM-Fe-PGCP are exemplified by SEM micrographs in Fig. 3. The CP displays intercellular gaps in the form of longitudinal cavities, which can be clearly marked as the unit cells are partially exposed. To hold the unit cells firmly in the CP fibers, the inter cellular gaps are filled by binder lignin and fatty substances. The size of the voids in original CP reduced after graft polymerization with acrylamide. It can be found that the surface of the AM-PGCP becomes much rougher than that of the CP. Like many polymer grafted lignocellulosic residues, AM-PGCP is also hydrophobic in nature (caused by MBA cross-links) and the porous structure provides new adsorption sites from inner cavities to participate in binding iron(III). The surface morphology of the AM-Fe-PGCP is different from the AM-PGCP. The voids present in the AM-PGCP are

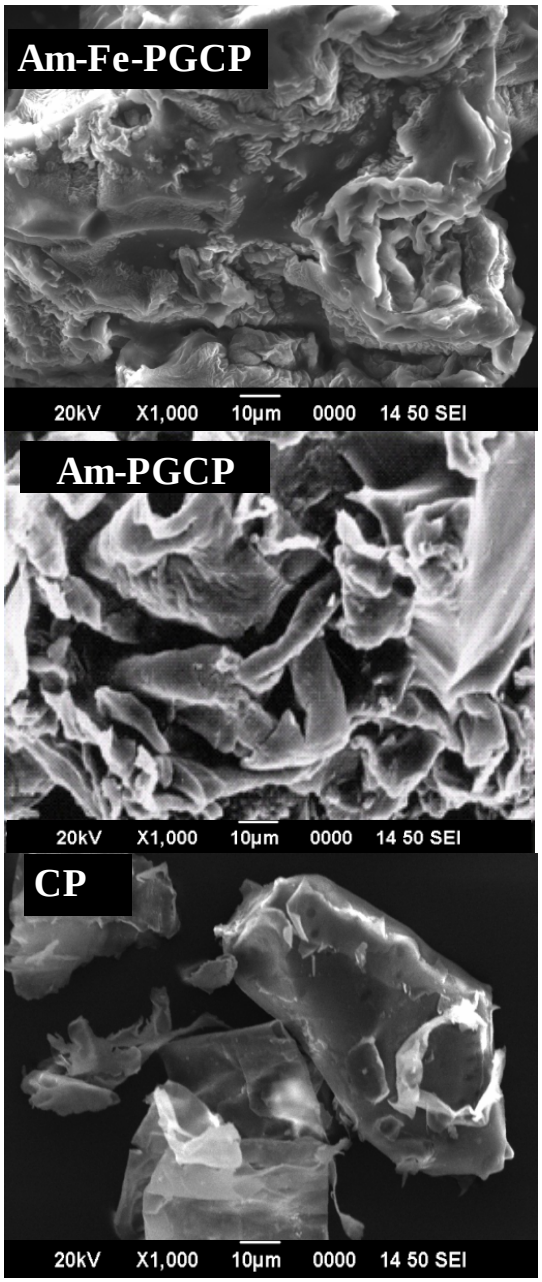

Fig. 3. SEM images of CP, AM-PGCP and AM-Fe-PGCP.

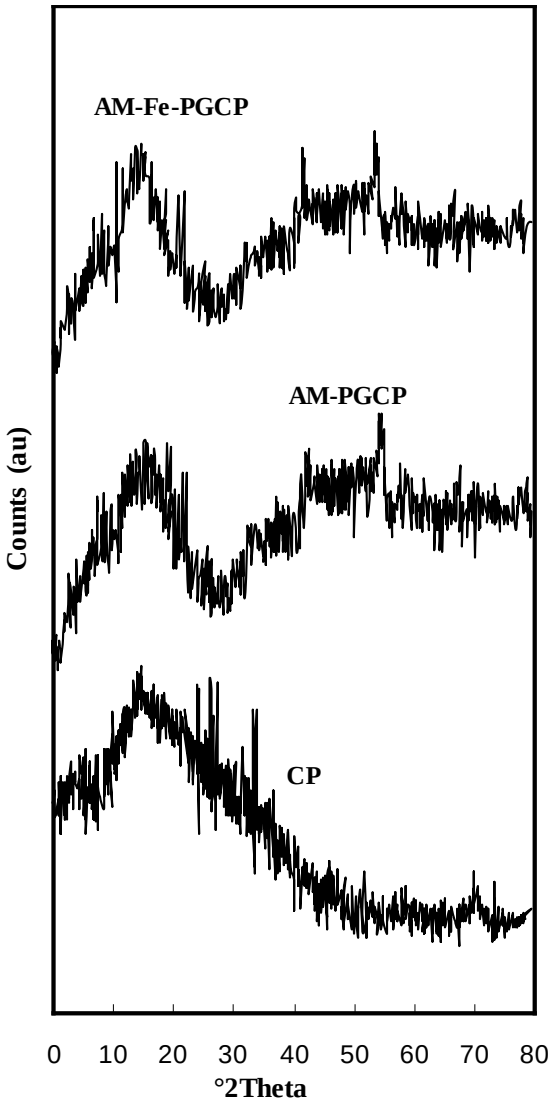

Fig. 4. X-ray diffraction patterns of CP, AM-PGCP and AM-Fe-PGCP.

not present in the iron(III) complexed AM-PGCP. This may be due to the contraction of the voids resulting from complexation or the disappearance of the voids during the rearrangement of polymer chains for complexation with iron(III).

The XRD patterns of CP, AM-PGCP and AM-Fe-PGCP are shown in Fig. 4. The XRD patterns of CP with 2 θ values 12.3, 19.4 and 21.8 assigned to the corresponding diffraction planes of ($1\bar{1}0$), (110) and (200) in the crystalline domain of cellulose structure. However in the XRD patterns of AM-PGCP, the only existence of peak at 2 θ = 19.4 and 21.8° indicates that some rearrangement in the morphology of cellulose chain occurs as a result of chemical modification. The decrease in intensity of peaks observed at 19.4° may be due to the phase transformation of cellulosic backbone. The basal spacing in CP decreases on modification indicates the reduction of tensile strength and crystalline domain in AM-Fe-PGCP. Therefore amine moieties protruded onto the aqueous medium and enhanced the adsorption ability of iron(III) on AM-PGCP (57.80 mg g^{-1}) which was higher than that of the original CP (29.97 mg g^{-1}). AM-Fe-PGCP shows new peaks centered at 2 θ = 26.1 and 33.3° indicating the presence of iron(III). It was observed that during the course of iron(III) loading on the AM-PGCP in aqueous solution there was a decrease in pH of the solution from about 3.0 to 1.2 at equilibrium. This indicates that H^+ ions are released into the solution with the complexation of iron(III). At a pH of

1.2, Fe^{3+} ions formed in the solution are complexed with amine and amide nitrogen from the adsorbent. The peak at 2 θ = 21.4° observed in the spectrum of AM-PGCP is shifted to a slightly higher angle by Fe^{3+} complexation, indicating the structural rearrangement of the material occurred during the course of complexation, in good agreement with the conclusion drawn from SEM images of the AM-Fe-PGCP.

Fig. 5 shows the TG and DTG curves of CP, AM-PGCP and AM-Fe- PGCP. The weight loss of the CP was around 70.3% in the heating process of up to 800°C. In the initial stage of decomposition (T_1 = 80°C) a weight loss of 5.9% was observed due to the decomposition of adsorbed water. In the second stage (T_2 = 332°C) 49.3% is lost due to the splitting of the cellulose structure and the chain scission and breaking of some carboxyl and carbonyl bonds in the ring structure evolving CO, CO_2 and water and condensed tar byproducts leaving behind rigid carbon skeleton. In the case of AM-PGCP, the initial decomposition temperature (T_1) is 85°C, where a weight loss 4.4% is observed due to the loss of adsorbed water. Second stage reaction between 180 and 410°C (T_2 = 346°C) where 40.2% of the dry weight loss is observed due to the release of water and CO_2 by the pyrolytic decomposition of cellulose unit and reorganization of carbon skeleton. In the third stage between 410 and 680°C (T_3 = 449°C) where 63.0% weight loss is observed due to the pyrolytic decomposition process in lignin and destruction of aminated fraction. The TG and DTG curves of AM-Fe-PGCP showed weight loss at four different temperature ranges with maximum decomposition temperatures 95°C (T_1), 386°C (T_2), 550°C (T_3) and 620°C (T_4). The first degradation is assigned to the dehydration (3.6%), the second degradation is attributed to the cellulose fraction (38.8%) and the third degradation is assigned to the aminated fraction of fibers (58.8%). The fourth degradation (60.8%) reveals the increased stability of AM-Fe-PGCP due to amination followed by iron(III) loading. The thermal stability of the AM-Fe-PGCP is much better than that of AM-PGCP. This indicates that some stable structures are formed in situ during the course of iron(III) loading and introduces thermal stability in the structure.

The pH of point of zero charge (pH_{pzc}) is defined as the pH at which surface charge density (σ_0) is zero. The values of σ_0 as a function of pH at 0.01M $NaNO_3$ for CP, AM-PGCP and AM-Fe-PGCP were determined by a potentiometric titration method [16]. The results are shown in Fig. 6. The point of intersection σ_0 with the pH curves gives the value of pH_{pzc}. The values of pH_{pzc} were found to be 6.0, 7.4 and 7.7 for CP, AM-PGCP and AM-Fe-PGCP, respectively. The increase in pH_{pzc} after polymer grafting and iron(III) loading indicates that the surface becomes more positive and this facilitates the electrostatic interaction with anions. A variation in anion exchange capacity (0.32 meq g^{-1} for CP, 0.43 meq g^{-1} for AM-PGCP and 0.73 meq g^{-1} for AM-Fe-PGCP) was also observed.

The adsorption isotherms of N_2 at 77 K on CP, AM-PGCP and AM-Fe-PGCP indicates that mesoporous texture of CP and the polymerization enhance to make a narrow range of micropores. The amount adsorbed decreases in the order: CP > AM-PGCP > AM-Fe-PGCP. The surface areas were calculated using the BET equation which is the most widely used procedure for determination of specific surface area. The total pore volumes were estimated to be the liquid volume of N_2 at a relative pressure of 0.99. The values of surface area were 84.2, 36.5 and 29.8 $m^2 g^{-1}$ for CP, AM-PGCP and AM-Fe-PGCP respectively; the corresponding values of pore volume were 0.42, 0.33 and 0.29 $cm^3 g^{-1}$. The amine content was determined by using the titration procedure and was found to be 2.38 meq g^{-1}.

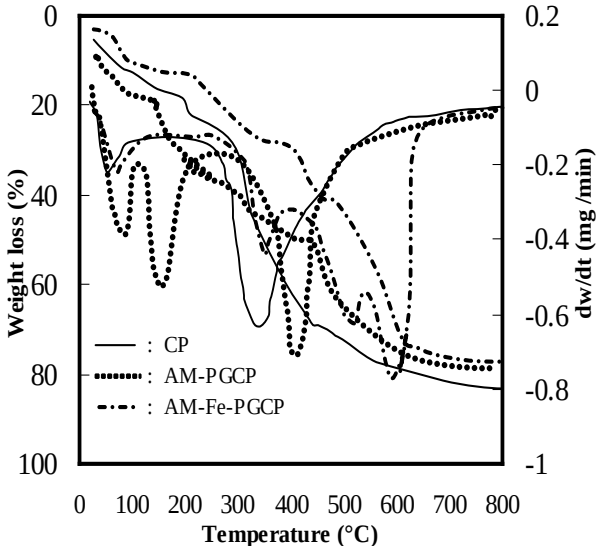

Fig. 5. TG and DTG curves of CP, AM-PGCP and AM-Fe-PGCP.

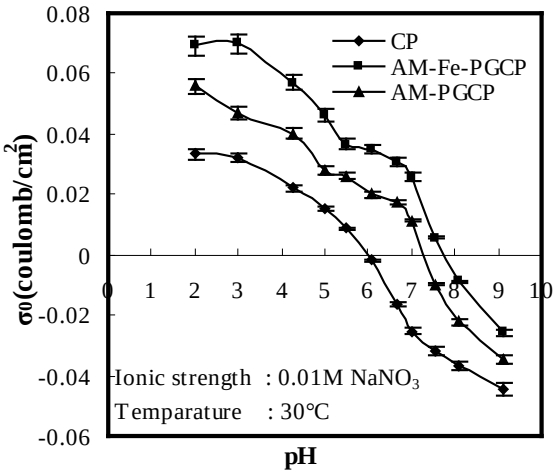

Fig. 6. Effect of surface charge density as a function of solution pH.

3.2. Effect of surface modification on Cr(VI) removal

The effect of surface modification on Cr(VI) removal was studied by conducting batch experiments using an initial concentration of 25 mg L^{-1} a with varying adsorbent dose of CP, AM-PGCP and AM-Fe-PGCP. Fig. 7 shows that the percentage adsorption increased with the increase in adsorbent doses and for the quantitative removal of 25 mg Cr(VI) from 1 L aqueous solution, a maximum adsorbent dosage of 5.5 g CP, or 3.5 g of AM-PGCP or 2.5 g AM-Fe-PGCP was required. The results clearly show that AM-Fe-PGCP was 2.2 and 1.4 times more effective than CP and AM-PGCP, respectively for Cr(VI) removal from aqueous solutions.

3.3. Effect of solid/liquid ratio on Cr(VI) removal

To study the effect of solid/liquid ratio on the adsorption capacity of the AM-Fe-PGCP for Cr(VI) removal, batch adsorption experiments were conducted for an initial Cr(VI) concentration of 150 mg L^{-1} and the adsorbent dose of 20–200 mg per 50 mL adsorption medium. The adsorption capacity of the AM-Fe-PGCP increased upto an optimum dosage, beyond which the extent of adsorption is increasing slowdown. An increase in the adsorbent dose from 20 to 100 mg in 50 mL adsorption medium led to an increase in adsorption from 36.6 to 95.8% and thereafter the extent of adsorption slowed down. The increase in the removal efficiency of the adsorbent with the increase in its dosage may be due to the increase in the number of adsorption sites. Thus, an optimum dosage of 100 mg AM-Fe-PGCP in 50 mL adsorption medium was used in subsequent adsorption experiments.

3.4. Effect of pH on Cr(VI) removal

The effect of pH on the adsorption of Cr(VI) onto AM-Fe-PGCP was studied by varying the pH from 2.0 to 10.0 using two different initial concentrations of 25 and 50 mg L^{-1} and the results are presented in Fig. 8. The results demonstrated that the adsorption percentage increased with pH and attained maximum at pH range 4.0–6.0, after which it showed a steady decrease. Cr(VI) ions present in the electroplating wastewater as in the forms of chromates (CrO_4^{2-}), dichromates ($Cr_2O_7^{2-}$), and bichromates ($HCrO_4^-$). Depending on pH and Cr concentration [18], the Cr(VI) species exist with equilibrium constant (at ambient conditions) as follows:

$$H_2CrO_4 \leftrightarrow H^+ + HCrO_4^-;\ pK_1 = 6.51 \quad (2)$$

$$2HCrO_4^{2-} \leftrightarrow Cr_2O_7^{2-} + H_2O;\ pK_2 = 5.65 \quad (3)$$

$$HCrO_4^- \leftrightarrow H^+ + CrO_4^{2-};\ pK_3 = 14.56 \quad (4)$$

At pH range 4.0–6.0, the dominant $HCrO_4^-$ species will adsorb on the positively charged surface of the AM-Fe-PGCP through the ion exchange process [19]. The $HCrO_4^-$ ions are exchanged with Cl^- ions from the adsorbent surface. The reaction can be represented as:

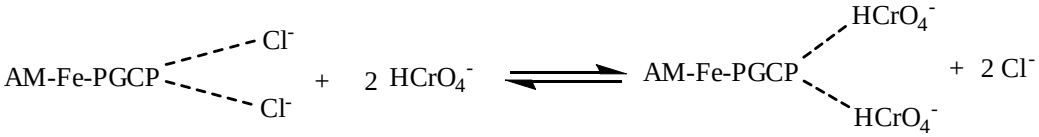

(5)

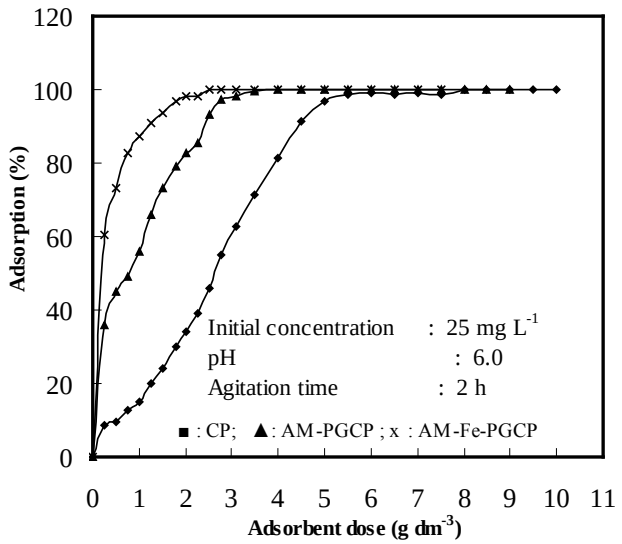

Fig. 7. Effect of surface modification on Cr(VI) removal.

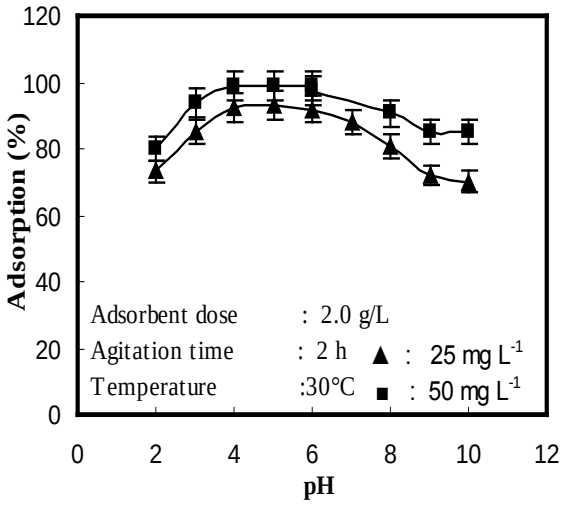

Fig. 8. Effect of pH on the adsorption of Cr(VI) onto AM-Fe-PGCP.

Low adsorption at higher pH values implies that CrO_4^{2-} ions compete with OH^- ions to the reaction sites of the adsorbent [19]. At lower pH values, $Cr_3O_{10}^{2-}$ and $Cr_4O_{13}^{2-}$ species are formed and these species are difficult to exchange with Cl^- ions from the adsorbent surfaces. The pH value less than 4.0 shows a decrease in adsorption even though the adsorbent surface is positively charged and sorbate species are negatively charged. In this case, chromate ions (H_2CrO_4) more protonated are less adsorbable than the less protonated one. In view of electrostatic interaction between the sorbent-sorbate systems, it was decided to maintain the pH at 4.0 subsequent adsorption experiments.

3.5. Effect of contact time and initial concentration

The effect of the contact time and initial concentration on the adsorption rate was studied using arrange of initial concentrations (100, 150, 200 and 250 mg L^{-1}) and the results are shown in Fig. 9. It is clear from Fig. 8 that the adsorption efficiency increases rapidly during the first 30 min and slowly reaches the saturation at about 2 h. After 120 min, the change of adsorption efficiency for Cr(VI) did not show notable effects. The initial concentration did not have a significant effect on the time to reach equilibrium. The adsorption equilibrium considered for the subsequent experiments has been taken as 2 h. The time profile of Cr(VI) uptake is a single, smooth and continuous curve leading to saturation, suggesting the cooperativity of Cr(VI) on the surface of the adsorbent. The equilibrium time of 2 h can be considered very short, which is an economically favorable condition for the adsorbent described here. The Cr(VI) adsorption capacity of AM-Fe-PGCP at equilibrium was 49.95 mg g^{-1} (99.6%), 74.91 mg g^{-1} (98.08%), 98.97 mg g^{-1} (96.9%) and 121.44 mg g^{-1} (97.2%) at an initial concentration of 100, 150, 200 and 250 mg/L, respectively. The results show that an increase in the initial Cr(VI) concentration leads to an increase in the Cr(VI) uptake. The important driving force to overcome all mass transfer resistance between solid–liquid phase was the initial concentration of adsorbed species. Hence a higher initial Cr(VI) concentration would enhance the adsorption process.

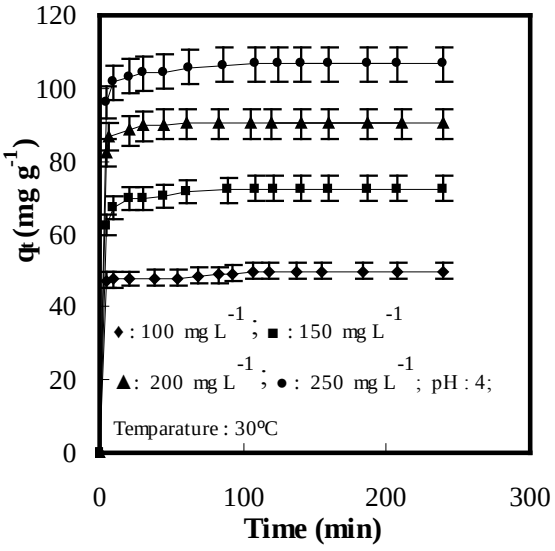

Fig. 9. The effect of contact time and initial concentration on the adsorption of Cr(VI) onto AM-Fe-PGCP.

3.6. Adsorption kinetics

In order to evaluate the kinetic mechanism that controls the adsorption process, Lagergren's pseudo-first-order, pseudo-second-order [20] and diffusion kinetic models were tested to interpret the experimental data. The pseudo-first-order kinetic model equation is represented by

$$q_t = q_e[1 - e^{(-k_1 t)}] \tag{6}$$

where q_t and q_e are the amount of adsorbate sorbed at time t and at equilibrium, respectively and k_1 is the pseudo-first-order rate constant (min^{-1}).

The pseudo-second-order kinetic model equation is expressed as:

$$q_t = \frac{k_2 q_e^2 t}{1 + k_2 q_e t} \tag{7}$$

where q_e is the maximum adsorption capacity (mg g^{-1}) and k_2 is the equilibrium rate constant for pseudo-second-order adsorption (g mg^{-1} min^{-1}). Modeling of kinetic data was performed by a nonlinear regression method that involves the Levenberg-Marquardt method [21]. Correlations of kinetic data are presented in Table 1. The correlation coefficient (R^2) and chi-square (χ^2) values of the pseudo-second-order equation for non-linear plots were $R^2 > 0.98$ and $\chi^2 < 1.23$ for the selected concentration range (100–250 mg L^{-1}) and temperatures (30–60°C), which suggests that the adsorption kinetics can be well described by the pseudo-second-order equation. The theoretical q_e values as calculated from pseudo-second-order kinetic model agree perfectly with the experimental q_e values (Fig. 9). This suggests that the adsorption of Cr(VI) onto AM-Fe-PGCP follows a pseudo-second-order kinetic model.

The influence of the initial concentration of Cr(VI) on the rate constant reveals the decreasing tendency of the rate which can be interpreted by the existence of Cr(VI) species in the solution. According to the equilibrium relationship [22], at lower initial concentration, $HCrO_4^-$ is the predominant species which can easily move towards the AM-Fe-PGCP surface. As the initial concentration increases the concentration of $HCrO_4^-$ ions increase but a less amount of $Cr_2O_7^{2-}$ ions also coexist along with $HCrO_4^-$ ions. Large sized $Cr_2O_7^{2-}$ ions (7.3×10^{-3} m^3/mol) move

Table 1
Kinetic parameters for the adsorption of Cr(VI) onto AM-Fe-PGCP at different temperatures and concentrations

Variable	Pseudo-first-order					Pseudo-second-order			
Temperature (°C)	q_e exp (mg g^{-1})	$k_1\times10^{-2}$ (min^{-1})	q_e cal (mg g^{-1})	R^2	χ^2	$k_2\times10^{-2}$ (g $mg^{-1}min^{-1}$)	q_e cal (mg g^{-1})	R^2	χ^2
20	98.01	1.75	10.28	0.90	3.7	0.98	97.14	0.99	0.05
30	104.28	1.77	16.36	0.95	5.2	1.02	105.10	0.99	0.31
40	111.87	2.14	17.17	0.96	6.4	1.84	109.53	0.99	0.61
50	115.27	2.51	28.71	0.92	4.5	2.10	115.29	0.99	1.23
Concentration (mg/L)									
100	49.95	0.9	9.80	0.87	5.6	5.6	49.09	0.98	0.92
150	74.99	1.1	13.5	0.89	7.6	2.6	72.71	0.99	0.79
200	98.80	1.2	18.4	0.92	9.5	1.3	96.97	0.99	0.25
250	121.50	1.4	33.5	0.91	4.6	0.7	118.44	0.99	1.01

slowly as compared with the small sized $HCrO_4^-$ (4.4×10^{-3} m^3/mol) [23]. Again, the inter electronic repulsive force increases with an increase in $Cr_2O_7^{2-}$ ion concentration, which retard the transport rate of $HCrO_4^-$ ion. Therefore, the value of rate constant decreases with the increase in initial Cr(VI) concentration.

The values of film diffusion coefficient (D_F) for the adsorption of Cr(VI) onto AM-Fe-PGCP were determined using the following expression

$$D_F = \frac{0.23 r_0 \delta}{t_{1/2}} \times \frac{\overline{C}}{C} \tag{8}$$

where r_0 is the radius of the adsorbent particle, $\overline{C}/C$ is the equilibrium loading of the adsorbent, and δ is the film thickness (10^{-3} cm). The values of D_F were found to be 3.65×10^{-7}, 4.10×10^{-7}, 4.28×10^{-7} and 4.45×10^{-7} cm^2 s^{-1} for an initial concentration of 100. 150, 200 and 250 mg L^{-1}, respectively. The D_F values at different temperatures were also calculated and were found to be 2.71×10^{-7}, 3.35×10^{-7}, 4.01×10^{-7} and 4.51×10^{-7} cm^2 s^{-1} at 30, 40, 50 and 60°C, respectively. Michelson [24] reported that the values of D_F should be in the range of 10^{-6}–10^{-8} cm^2 s^{-1} for film diffusion controlled adsorption process. Since the values obtained for D_F are in the order of 10^{-7} cm^2 s^{-1}, it may concluded that the process of Cr(VI) adsorption onto AM-Fe-PGCP is controlled by film diffusion process.

3.7. Adsorption isotherm study

To optimize the design of an adsorption system for the adsorption of a solute, it is important to establish the most appropriate correlation for the equilibrium curves. Adsorption isotherms of Cr(VI) onto AM-Fe-PGCP at differential temperatures are shown in Fig. 10. The Langmuir

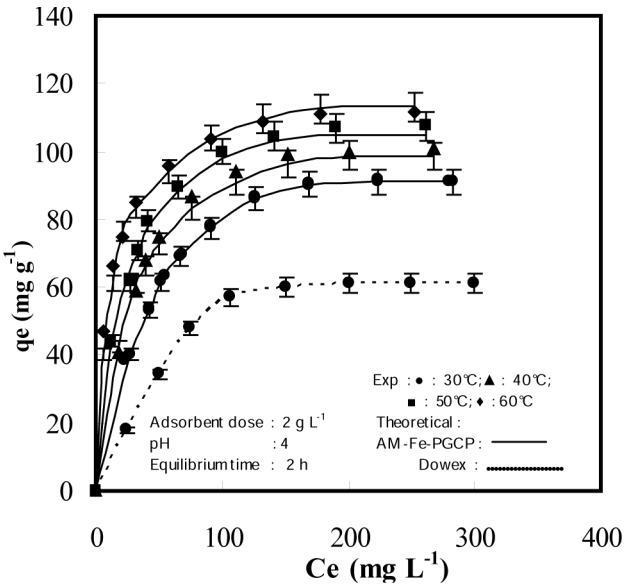

Fig. 10. Comparison of experimental and simulated model fits of the isotherm for the adsorption of Cr(VI) onto AM-Fe-PGCP at different temp and Dowex MWA1.

and Freundlich isotherm models were used to describe the equilibrium characteristics of adsorption. The mathematical expression of the Langmuir model is

$$q_e = \frac{Q_0 b C_e}{1 + bC_e} \tag{9}$$

where q_e is the amount adsorbed (mg/g) and C_e is the adsorbate concentration in solution (mg L^{-1}), both at equilibrium. Q_o is the monolayer capacity of the adsorbent (mg g^{-1}) and b is the energy of adsorption (L mg^{-1}). A basic assumption in the Langmuir theory is that adsorp-

tion takes place at specific homogeneous sites within the adsorbent [25]. The empirical Freundlich expression is an exponential equation and therefore, assumes that as the adsorbate concentration increases so too does the concentration of adsorbate on the adsorbent surface. The Freundlich adsorption isotherm can be expressed [26] as:

$$q_e = K_F C_e^{1/n} \tag{10}$$

where K_F is the Freundlich adsorption constant which is a comparative measure of the adsorption capacity of the adsorbent and $1/n$ is an empirical constant indicates the intensity of the adsorption. The magnitude of n values gives an indication of the favorability of the adsorbent/adsorbate system. Values of $n > 1.0$ are usually termed as favorable adsorption.

The isotherm parameters were calculated using nonlinear regression analysis and the results are shown in Table 2. It is obvious that the Cr(VI) sorption capacity of AM-Fe-PGCP increased with the rise in temperature, and high capacity was observed at 60°C. The values of R^2 and χ^2 show that the adsorption process is fitted to the Langmuir and Freunlich equation, of which the former gives the best correlation indicating monolayer adsorption process. Fig. 10 shows the comparative fit of the Langmuir and Freunlich isotherms with equilibrium data, and it is again clear from the figure that the Langmuir isotherm shows a very good fit with data. Favorability of adsorption was further checked by using a dimensionless separation factor (R_L). The R_L values are in the order $0 < R_L < 1$, $R_L > 1$, $R_L = 1$ and $R_L = 0$ indicates favorable, unfavorable, linear and irreversible, respectively for the conditions with the shape of isotherms. The values of R_L for the adsorption of Cr(VI) were calculated at different concentrations (100–600 mg L^{-1}) and temperatures (30–60°C) and were found to be in the range 0.02–0.17. This indicates that the adsorption process is favorable and the adsorbent employed is exhibited a high adsorption potential.

3.8. Thermodynamic study

The temperature dependency onto rate is important to predict the feasibility of the reaction. The nonlinear regression represents a good fit over the entire range of temperatures (30, 40, 50 and 60°C) for pseudo-second-order analysis (Table 1). The energy of activation (E_a) for the adsorption process was calculated using the following Arrhenius equation:

$$\ln k_2 = \ln A - \frac{E_a}{RT} \tag{11}$$

where k_2 is rate constant, and A is the Arrhenius factor. To extract, the values of A and E_a were determined from the intercept and slope of ln k vs. $1/T$ plot (Fig. 11). The values of A and E_a were calculated from the intercept and slope of the plot and were found to be 88.63 L mol^{-1} s^{-1} and 22.37 kJ mol^{-1}, respectively. The E_a values within the energy range 0–40 kJ mol^{-1}. Then, the type of adsorption of Cr(VI) onto AM-Fe-PGCP according to the value obtained is physical [27]. The values of the entropy of activation (ΔS^*) and enthalpy of activation (ΔH^*) were also determined from the intercept and the slope of the linear plot according to Eyring equation:

$$\ln\left(\frac{k}{T}\right) = \ln\left(\frac{k_b}{h}\right) + \frac{\Delta S^*}{R} - \frac{\Delta H^*}{RT} \tag{12}$$

where k_b and h are Boltzmann's and Planck's constants, respectively. According to Eq. (11), a plot of ln (k/T) vs. $1/T$ should be a straight line with a slope $\Delta H^*/R$ and in-

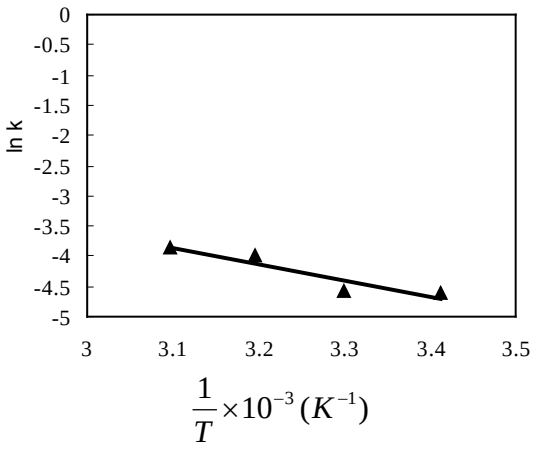

Fig. 11. ln k vs. $1/T$ plot for the adsorption of Cr(VI) onto AM-Fe-PGCP.

Table 2
Langmuir and Freundlich isotherm constants for the sorption of Cr(VI) onto AM-Fe-PGCP

Temperature (°C)	Langmuir				Freundlich			
	Q_0 (mg g^{-1})	b (L mg^{-1})	R^2	χ^2	K_F (mg g^{-1})	n	R^2	χ^2
30	135.5	0.04	0.99	0.22	25.6	3.4	0.95	10.4
40	149.8	0.07	0.98	0.34	43.9	4.6	0.95	11.2
50	158.7	0.12	0.98	0.16	56.4	5.2	0.94	9.23
60	175.4	0.14	0.99	0.51	60.5	5.4	0.93	11.2

tercept [ln (k_b/h) + $\Delta S^*/R$]. Gibbs free energy of activation (ΔG^*) may be written in terms of entropy and enthalpy of activation:

$$\Delta G^* = \Delta H^* - T\Delta S^* \quad (13)$$

The value of ΔG^* was calculated at 303 K from Eq. (10). The values of ΔG^*, ΔH^* and ΔS^* of activation were found to be 85.03 kJ mol^{-1}, 18.37 kJ mol^{-1} and –220.00 J mol^{-1} K^{-1}, respectively. The positive values of E_a, and ΔG^* suggest the existences of the energy barrier in the exchange reactions. $\Delta G^* > 0$, which means the adsorption of Cr(VI) ions on AM-Fe-PGCP is nonspontaneous and need additional energy to complete the adsorption process. Positive value of ΔH^* suggests that the adsorption process is endothermic in nature and this is supported by the increases of Cr(VI) adsorption onto AM-Fe-PGCP with a rise in temperature, as shown in Fig. 9. The negative ΔS^* value indicates that as a result of adsorption, no significant change occurs in the internal structure of the exchanger [28]. The negative value of ΔS^* also indicates that the Cr(VI) ions at AM-Fe-PGCP are always more organized than those in the bulk solution. It was found that $\Delta H^* > -T\Delta S^*$. This indicates that the influence of enthalpy is more remarkable than entropy of activation. The heat of adsorption determined at constant amount of adsorbate adsorbed is known as isosteric heat of adsorption (ΔH_x) and its magnitude can be measured experimentally by using Clausius–Clapeyron equation [29]:

$$\frac{d(\ln Ce)}{dt} = \frac{-\Delta H_x}{RT^2} \quad (14)$$

The plots of ln C_e vs. 1/T (figure not shown) for different amounts of Cr(VI) adsorption were found to be linear and the values of ΔH_x were measured from the slopes of the plots. The values of ΔH_x were found to remain almost constant (≈51.59 kJmol^{-1}) with the increase in surface loading from 30.00 to 70.00 mg g^{-1}. This indicates that the surface of AM-Fe-PGCP is energetically more or less homogeneous and the lateral interactions between adsorbed Cr(VI) ions do not exist.

3.9. Test with simulated industrial wastewater and comparative study with synthetic ion exchanger

The simulated wastewater was prepared and treated with AM-Fe-PGCP to demonstrate the adsorption potential and utility in removing Cr(VI) from wastewater in the presence of other ions. The composition of the wastewater [30] is: Cr(VI) 27.7 mg L^{-1}; Cd(II) 3.8 mg L^{-1}; CN^- 12.5 mg L^{-1}; Ni(II) 5.1 mg L^{-1}; Cu(II) 28.7 mg L^{-1}; Zn(II) 4.2 mg L^{-1}; chemical oxygen demand 160.4 mg L^{-1}; biological oxygen demand 49.7 mg L^{-1}, suspended solids 412.5 mg L^{-1} and pH 4.3. The effect of the adsorbent dose on Cr(VI) removal was studied. It is evident that for the quantitative removal of Cr(VI) from 1.0 dm^3 wastewater contain 27.7 mg L^{-1} and several other ions; an adsorbent dosage of 0.5 g L^{-1} is sufficient for the removal of 99.8% of the total Cr(VI). The efficiency of the adsorbent for the adsorption of Cr(VI) from wastewater is not significantly different from the results predicted on the batch experiments using Cr(VI) only. Under these conditions the lowest Cr(VI) concentration attained by this material was 0.05 mg L^{-1}. The permissible limit of the Cr(VI) for the discharge of industrial wastewater is 0.20 mg L^{-1}.

The experimental isotherm data obtained for AM-Fe-PGCP at pH 4.0 and at 30°C were compared with a commercial synthetic polymer based anion exchanger. For this, a commercial chloride — form weak base styrene-DVB based anion exchanger, DOWEX MWA-1 obtained from Aldrich Chemicals Co. USA was used. It has tertiary amine functionality with an anion exchange capacity of 1.3 meq L^{-1}. Experimental isotherm data are shown in Fig. 10. The values of $Q°$ and b were determined by a non- linear regression analysis and were found to be 113.87 mg/g and 0.07 L/mg, respectively. In the present study, the adsorption capacity of AM-Fe-PGCP has also been compared with that of other adsorbents based on their maximum monolayer adsorption capacity for Cr(VI). The $Q°$ values for the adsorption of Cr(VI) onto activated carbon, eucalyptus bark, chitosan and ethylenediamine-modified rice hull [31–34] were reported to be 125.5, 45.0, 50.0 and 23.4 mg g^{-1}, respectively. The differences of Cr(VI) uptake on various adsorbents are due to the properties (functional groups, surface area, particle size, porosity, etc.) of the adsorbents. The amount of adsorbed Cr(VI) at 30ºC was high enough for AM-Fe-PGCP (135.5 mg g^{-1}) to be able to effectively remove Cr(VI) from wastewater.

3.10. Desorption and regeneration studies

Since Cr(VI) adsorption onto AM-Fe-PGCP is a reversible process, it is possible for regeneration or activation of the adsorbent to reuse. The primary objective of regeneration is to restore the adsorption capacity of exhausted adsorbent while the secondary objective is to recover valuable components present in the adsorbed phase. The adsorption of Cr(VI) on AM-Fe-PGCP is highly pH dependent, hence the desorption of Cr(VI) was possible by controlling the pH. Attempts were made to desorb Cr(VI) ions from spent adsorbent with various eluents such as NaOH, Na_2SO_4, NaCl and $NaNO_3$.The desorption efficiency of 0.1 M solution of NaOH, NaCl, $NaNO_3$ and Na_2SO_4 was found to be 96.6, 81.7, 62.3 and 47.3%, respectively. Among these eluents 0.1 M NaOH possesses superior desorpion capacity.

Desorption of Cr(VI) from AM-Fe-PGCP was 67.4, 72.5, 78.8, 85.6 and 96.6% with 0.001, 0.005, 0.01, 0.05 and 0.1 M NaOH, respectively. From these results it may be concluded that ligand exchange occurs in the adsorption process. The results of regeneration study of Cr(VI) by 0.1 M NaOH solution (equilibrium pH 12.0–12.5) are

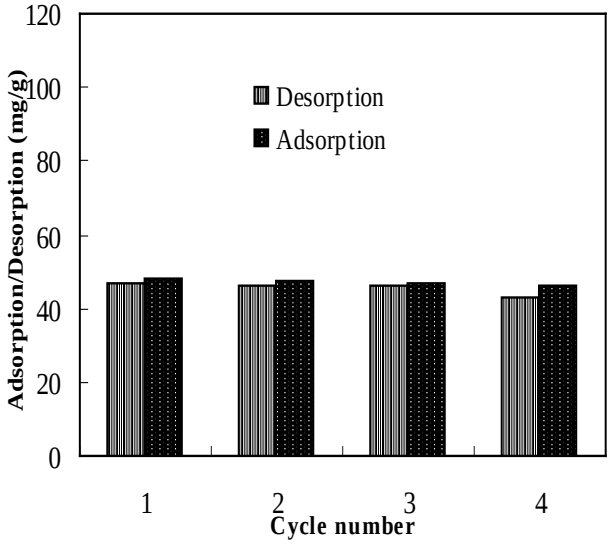

Fig. 12. Four cycles of Cr(VI) adsorption–desorption with 0.1 M NaOH as the desorbing agent.

shown in Fig. 12. After four cycles the adsorption capacity of AM-Fe-PGCP decreased from 48.27 mg g^{-1} (96.6%) to 46.10 mg g^{-1} (92.2%), while the recovery of Cr(VI) decreased from 46.87 mg g^{-1} (97.1%) in the first cycle to 43.20 mg g^{-1} (93.7%) in the fourth cycle. After each desorption experiments we re-introduced Fe^{3+} to restore the adsorption sites, almost the same as the original values and subsequent adsorption experiments were conducted using re-introduced Fe^{3+} in AM-Fe-PGCP (AM-re-Fe-PGCP). The amount of Fe^{3+} restored in the regenerated adsorbent after removal of Cr(VI) by NaOH treatment was 8.7, 9.5, 9.8 and 8.4 mg g^{-1} in the first, second, third and fourth cycle, respectively. The regenerated adsorbent showed uptake efficiency comparable to that of the fresh ones over four cycles. The results show that even after four cycles of adsorption and desorption there was no appreciable decrease in the sorption capacity of AM-Fe-PGCP. This indicated that the material could be reused for 4–5 times for the sorption of Cr(VI).

4. Conclusions

The graft copolymerization of acrylamide monomer in the presence of N,N′-methylene bisacrylamide onto a lignocellulosic residue (coconut coir pith) was carried out by the peroxydisulphate induced free radical initiated polymerization method. Surface characterization was done by using FTIR, SEM, XRD, TG/DTG, surface area analyzer, and potentiometric titrations. Removal of Cr(VI) greater than 99.0% was achieved under optimum conditions. The kinetics of the sorption process was found to follow the pseudo-second-order rate law. The adsorption increases with increasing temperature. Eyring equation was used to calculate the thermodynamic constants. The isotherm data were correlated well by Langmuir model as compared to Freundlich isotherm model. This adsorbent exhibited high adsorption capacity, the maximum adsorption capacity for Cr(VI) was 135.5 mg g^{-1} at 30ºC. Quantitative removal of 27.7 mg L^{-1} Cr(VI) in 1.0 L of electroplating industry wastewater was achieved by 0.5 g L^{-1} of the adsorbent at pH 4.3 and 30°C. The alkali treatment (0.1 M NaOH) and re-incorporation of Fe^{3+} led to a reactivation of the used adsorbent and the adsorbent could be reused for several cycles, consecutively without noticeable loss of capacity. The results of this study suggest that AM-Fe-PGCP exhibits significant potential as an adsorbent in the removal of Cr(VI) from aqueous solutions and industrial wastewaters.

Acknowledgements

The authors are thankful to the Head of Department of Chemistry, University of Kerala, Trivandrum for providing laboratory facilities, and Mr. S. Rijith expresses his sincere thanks to the University Grants Commission, New Delhi for the financial support in the form of Research Fellowship to carry out this work.

References

[1] S. Chiarle, M, Ratto and M. Rovatti, Water Res., 34 (2000) 2971–2978.
[2] Environmental Protection Agency (EPA), http://www.epa.gov.
[3] J.R. Gardea-Torresday, G. de la Rosa and J.R. Peralta-Videa, Pure Appl.Chem., 76 (2004) 801–813.
[4] S. Babel and T.A. Kurniawan, J. Hazard. Mater., B97 (2003) 219–243.
[5] T.S. Anirudhan and P.G. Radhakrishnan, J. Chem. Thermodynamics, 40 (2008) 702–709.
[6] R. Saliba, H. Gauthier, R. Guathier and M. Petit-Ramel, J. Appl. Polym. Sci., 75 (2000) 1624–1631.
[7] D. Mohan and C.U. Pittman, J. Hazard. Mater., 142 (2007) 1–53.
[8] M.N. Amin, S. Kaneco, T. Kitagava, A. Begum, H. Katsumata, T. Suzuki and K. Ohta, Ind. Eng. Chem. Res., 45 (2006) 8105–8110.
[9] I.G. Shibi and T.S. Anirudhan, J. Chem. Technol. Biotechnol., 81 (2006) 433–444.
[10] B.F. Noelin, D.M. Manohar and T.S. Anirudhan, Separ. Purif. Technol., 45 (2005) 131–140.
[11] M. Gopal and R.A. Gupta, Indian Coconut J., 31 (2000) 13–16.
[12] T.S. Anirudhan and M.R. Unnithan, Chemosphere, 66 (2007) 60–66.
[13] T.S. Anirudhan, L. Divya and P.S. Suchithra, J. Env. Manage., 90 (2009) 549–560.
[14] E. Ott, Cellulose and Cellulose Derivatives, Interscience Publishers, NewYork, 1946.
[15] T.S. Anirudhan, M.R. Unnithan, L. Divya and P. Senan, J. Appl. Polym. Sci., 104 (2007) 3670–3681.
[16] J.A. Schwarz, C.T. Driscoll and A.K. Bhanot, J. Colloid. Interface Sci., 97 (1984) 55–61.
[17] A.E. Greenberg, L.S. Clescerl and A.D. Eaton, Standard Method for the Examination of Water and Wastewater, 18th ed., APHA, AWWA and WEF, Washington, D.C., 1992.
[18] J. Kotaś and Z. Stasicka, Environ. Poll., 107(3) (2000) 263–283.
[19] N.K. Hamadi, X.D. Chen, M.M. Farid and M.G.Q. Lu, Chem. Eng. J., 84 (2001) 95–105.
[20] T.S. Anirudhan and P.S. Suchithra, Ind. Eng. Chem. Res., 46

(2007) 4606–4613.
[21] D.W. Marquardt, J. Soc. Ind .Appl. Math., 11 (1963) 431–441.
[22] G. Cimino and A. Passerini, Water Res., 34 (2000) 2955–2962.
[23] F. Brito, J. Ascanio, S. Mateo, C. Hernandez, L. Araujo, P. Gili, P. Martin-Zarza, S. Dominguez and A. Mederos, Polyhedron, 16 (1997) 3835–3846.
[24] L.D. Michelson, P.G. Gideon, E.G. Pace and L.H. Kutel, US Department of Industry, Office of Water Resource and Technology, 1975, vol. 74.
[25] J.D. Seader and E.J. Henley, eds., Separation Process Principles; John Wiley & Sons, New York, 1998.
[26] H.M.F. Freundlich, Z. Phys. Chem., 57 (1906) 385–395.
[27] A. Mellah, S. Chegrouche and M. Berkat, J. Colloid. Interface Sci., 296 (2006) 434–441.
[28] D.C. Sharma and C.F. Forster, Process Biochem., 30 (1995) 293–298.
[29] D.M. Young and A.D. Crowell, Physical Adsorption of Gases. London, Butterworth, 1962.
[30] R. Maya, V.P. Vinod and T.S. Anirudhan, Ind. Eng. Chem. Res., 43 (2004) 2247–2255.
[31] H. Zghida, M.H.V. Baouab and R. Gauthier, J. Appl. Polym. Sci., 87 (2003) 1660–1665.
[32] V. Sarin and K.K. Pant, Bioresource Technol., 97 (2006) 15–20.
[33] R. Schmuhl, H.M. Krieg and K. Keizer, Water SA, 27 (2001) 1–8.
[34] P.L. Tang, C.K. Lee, K.S. Low and Z. Zainal, Environ. Technol., 24 (2003) 1243–1251.